Perturbation parameters associated with nonlinear responses of the head at small amplitudes

S. Gurses
Sensory Motor Performance Program, Rehabilitation Institute of Chicago, Chicago, Illinois 60611

Y. Dhaher[a)]
Sensory Motor Performance Program, Rehabilitation Institute of Chicago, Chicago, Illinois 60611 and Department of Physical Medicine and Rehabilitation, Feinberg School of Medicine, Northwestern University, Chicago, Illinois 60611

T. C. Hain
Department of Physical Therapy and Human Movement Science, Northwestern University, Chicago, Illinois 60611

E. A. Keshner
Sensory Motor Performance Program, Rehabilitation Institute of Chicago, Chicago, Illinois 60611 and Department of Physical Medicine and Rehabilitation, Feinberg School of Medicine, Northwestern University, Chicago, Illinois 60611

(Received 10 August 2004; accepted 28 April 2005; published online 14 June 2005)

The head–neck system has multiple degrees of freedom in both its control and response characteristics, but is often modeled as a single joint mechanical system. In this study, we have attempted to quantify the perturbation parameters that would elicit nonlinear responses in a single degree-of-freedom neuromechanical system at small amplitudes and velocities of perturbation. Twelve healthy young adults seated on a linear sled randomly received anterior–posterior sinusoidal translations with ±15 mm and ±25 mm peak displacements at 0.81, 1.76, and 2.25 Hz. Head angular velocity and angular position data were examined using a nonlinear phase-plane analysis. Poincaré sections of the phase plane were computed and Lyapunov exponents calculated to measure divergence (chaotic behavior) or convergence (stable behavior) of system dynamics. Variability of head angular position and velocity across the entire phase plot was compared to that of the Poincaré sections to quantify spatial–temporal irregularity. Multiple equilibrium points and positive Lyapunov exponents revealed chaotic behavior at 0.81 Hz at both amplitudes whereas responses at 1.76 and 2.25 Hz exhibited periodic oscillations, clustered phase points, and negative Lyapunov exponents. However, intersubject variability increased at the lowest frequency and a few subjects presented chaotic behavior at all frequencies. An inverted pendulum with position and velocity threshold nonlinearity was adopted as a simplistic model of the head and neck. Simulations with the model resulted in features similar to those observed in the experimental data. Our principal finding was that increasing the perturbation amplitude had a stabilizing effect on the behavior across frequencies. Nonlinear behaviors observed at the lowest stimulus frequency might be attributed to fluctuations in control between the multiple sensory inputs. Although this study has not conclusively pointed toward any single mechanism as responsible for the responses observed, it has revealed clear directions for further investigation. To examine if changing the sensory modalities would elicit a significant change in the nonlinear behaviors observed here, further experiments that target a patient population with some sort of sensory deficit are warranted. © *2005 American Institute of Physics*. [DOI: 10.1063/1.1938347]

The head–neck system has multiple degrees of freedom in both its control and response characteristics, but is often modeled as single joint mechanical system.[1] Linear system identification techniques associated with small amplitude perturbations are most often employed to understand the nature of the dynamics and control strategies that the central nervous system uses even with complex motor systems. However, we observed that the system does not behave in a linear fashion even around its equilibrium point. Crossing above and below the sensor thresholds could explain the emergence of nonlinear behaviors in response to small amplitude perturbations. In general, a system with inherent nonlinearities can exhibit various kinds of dynamics with respect to input and system parameter values. This puts an extra burden on the central controller to adjust the parameter values with respect to a given task to be performed. By this study, we propose that nonlinear system identification techniques should be used in order to get a reasonable insight to functional head–neck dynamics and control as well as

[a)]Author to whom correspondence should be addressed. Electronic mail: y-dhaher@northwestern.edu; Fax: 312-238-2208.

constructing an analytical basis for pathological cases.

I. INTRODUCTION

Head stabilization behavior has mostly been studied using linear systems techniques.[1–7] Although the head and neck has been modeled as a linear system,[8,9] it is clear that there are nonlinearities in this behavior that depend upon the nature of the stimulus content. The question we have asked here is not whether nonlinear behavior may exist, but how do we associate specific perturbation properties with quantified measures of nonlinear behavior?

The influence of particular stimulus parameters on system behavior may depend upon the biomechanical and neurophysiological origins of the specific nonlinearity. Motor system nonlinearities can originate from both the intrinsic musculoskeletal mechanics as well as from the input/output properties of the sensors (i.e., threshold and gains). To experimentally identify if a nonlinearity exists, we have to be aware that even nonlinear systems can behave fairly linearly at well defined perturbation speeds and amplitudes. For example, if the amplitude of perturbation is less than the threshold of the sensor, then the sensor's nonlinear properties will not contribute to the overall response of the system.[10–13] Gravitational torque will produce linear mechanical behavior at a joint as a function of the angle if the angular deviations are small, but this behavior becomes more nonlinear as angular deviation increases.[14] Input dynamics, such as increasing perturbation speed (as occurs with increasing frequencies), are manifested as increased joint movement velocity and produce changes in the sensitivity of a receptor (e.g., nonlinear spindle dependence on velocity[15]).

In the present study we sought to determine to what extent nonlinear behaviors emerged in sagittal head movements that were elicited by precisely controlled linear perturbations. We have designed an experimental paradigm to elicit nonlinear behaviors in the head–neck system that have been assumed to be unimportant or of minimal impact at low amplitudes and velocities of perturbation. Dynamic response characteristics of the system were analyzed in the time and frequency domain. To establish whether the system behaved in a nonlinear fashion in response to the positional perturbations, nonlinear analyses of system behavior were performed using Poincaré sections and Lyapunov exponents. The stabilizing effect of the perturbation properties (frequency and amplitude) on the nonlinear head and neck dynamics was further investigated by examining the sign of the Lyapunov exponents both across amplitudes for all frequencies and within amplitudes across frequencies.

II. MATERIALS AND METHODS

A. Subjects

Twelve healthy young adults (7 females and 5 males aged 18–25 yrs) were studied. They had no known musculoskeletal injuries or neurological disorders that might have affected their ability to stabilize their head in space. All subjects gave written consent approved by the Internal Review Board at Northwestern University before undergoing the experimental protocol.

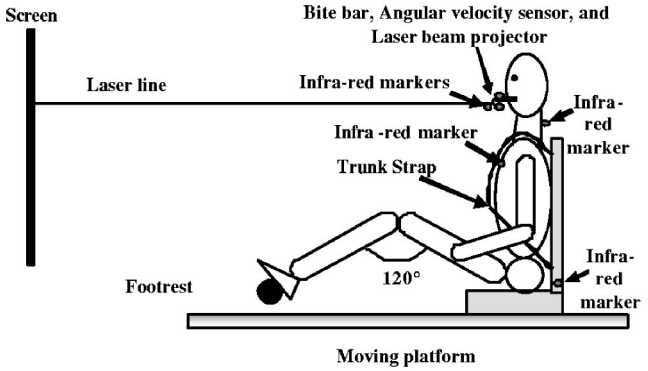

FIG. 1. An illustration of the position of the subject seated on the linear sled, the location of the infrared markers and the angular velocity sensor, and the direction of the laser beam projected on to the screen in front of the subject.

B. Apparatus

Subjects were seated in a rigid aluminum seat that provided support to the whole body with their legs partially extended and the knees raised (Fig. 1). A footrest that could be moved forwards and backwards was positioned so that all subjects had an angle between their thigh and calf of 120°. The seatback was almost orthogonal to the seatbase. The seatback and seatbase was firm and not supported by any kind of padding. The chair was bolted to a welded steel frame (sled) obtained from a "bumper-car" manufacturer (JJ-amusements, Salem OR). The sled was bolted to a high acceleration (2 g maximum), servo-controlled linear motor (Kollmorgan model IC55-100, Hauppauge, NY). A motion controller board (Galil DMC 1810-16, Rocklin, CA) controlled the sled motion. A five-point racing harness secured the subject firmly to the chair and minimized relative movement between the torso and the seat.

An individualized bite-bar was made using dental impression material (Paddan and Griffin[16]). Attached to the bite-bar with a total mass of 90 g was a small LED laser that projected a horizontal line, an angular rate sensor oriented to measure angular velocity in pitch (ARS-C141-1ARP, Watson Inc., Eau Claire, WI), and three infrared markers used by the 3-camera motion analysis system (CODAmotion, Charnwood Dynamics, United Kingdom) to record head angular position in space. Additional infrared markers were attached to the sternum, C7, and the sled (Fig. 1).

C. Procedures

Prior to each experiment, a plumb line and protractor was used to position the head so that the line between the external ear canal and inferior orbital rim was perpendicular to gravity. This angular head position was chosen to offset the angle which the canals make with the gravity vertical and start the subjects from the same initial angular position. Then, head roll position was adjusted by determining that the line projected from the head-mounted laser on to a transversal plane (screen) 2.5 m away from the subject was 0° with the Earth horizontal. Once this "horizontal" position was obtained, the position of the projected laser line was marked on the screen so that the head could be realigned by the subject

TABLE I. Quantified measures of the system in response to specific perturbation parameters.

Stimulus frequency (Hz)	Stimulus amplitude (mm)/ peak velocity (mm/s)/ peak acc (g)	RMS head angular velocity (deg/s)	Head magnitude wrt trunk displacement (deg/cm)	Phase of head wrt trunk (deg)	SD across the trial[a]	SD of Poincaré sections[a]
0.81	15/76/0.04	14±4	0.19±0.12	36±84	pos=1±0.4 vel=2.4±0.6	pos=1±0.4 vel=1.9±0.4[j]
1.76	15/166/0.19	26±8[b]	1.45±0.77[f]	29±14	pos=2.5±0.8 vel=19±10	pos=1.7±0.3[j] vel=6.8±2.6[j]
2.25	15/212/0.31	39±13[c]	1.85±0.77[g]	27±12	pos=3.1±1.3 vel=34±15	pos=2±0.9[j] vel=12±4.5[j]
0.81	25/127/0.07	14±4	0.21±0.09	46±44	pos=1.3±0.4 vel=3.6±1.1	pos=1.2±0.4 vel=2.6±0.8[j]
1.76	25/276/0.3	34±15[d]	1.28±0.71[h]	28±12	pos=3.4±1.5 vel=28±17	pos=2.1±0.6[j] vel=9.1±3.1[j]
2.25	25/353/0.51	52±22[e]	1.54±0.71[i]	24±12	pos=4.3±1.8 vel=47±24	pos=2.5±0.8[j] vel=21±9.1[j]

[a]N.B. pos=Mean±the standard deviation (SD) of head angular displacement across all subjects; vel=mean±the standard deviation of head angular velocity across all subjects.
[b]RMS head angular velocities are significantly different for 0.81 Hz stimulus compared to 1.76 Hz ($p<0.004$) at 15 mm peak displacement amplitude.
[c]RMS head angular velocities are significantly different for 0.81 Hz stimulus compared to 2.25 Hz ($p<0.000$) at 15 mm peak displacement amplitude.
[d]RMS head angular velocities are significantly different for 0.81 Hz stimulus compared to 1.76 Hz ($p<0.003$) at 25 mm peak displacement amplitude.
[e]RMS head angular velocities are significantly different for 0.81 Hz stimulus compared to 2.25 Hz ($p<0.000$) at 25 mm peak displacement amplitude.
[f]Transfer function magnitudes are significantly different for 0.81 Hz stimulus compared to 1.76 Hz ($p<0.000$) at 15 mm peak displacement amplitude.
[g]Transfer function magnitudes are significantly different for 0.81 Hz stimulus compared to 2.25 Hz ($p<0.000$) at 15 mm peak displacement amplitude.
[h]Transfer function magnitudes are significantly different for 0.81 Hz stimulus compared to 1.76 Hz ($p<0.000$) at 25 mm peak displacement amplitude.
[i]Transfer function magnitudes are significantly different for 0.81 Hz stimulus compared to 2.25 Hz ($p<0.000$) at 25 mm peak displacement amplitude.
[j]Poincaré sections were significantly different from the full data set at $p<0.05$ when corrected for multiple *t*-tests (12 comparisons for a corrected (Bonferroni adjustment) significance level at $p<0.004$).

prior to each trial. Both the initial pitch and roll angles of the head were controlled in this way. The laser was automatically turned off when the trial began. Subjects were instructed to hold their head erect while looking ahead with their eyes open. Six 180 s trials of sinusoidal inputs were randomized for three frequencies (0.81, 1.76, and 2.25 Hz) and two perturbation amplitudes (15 and 25 mm). The selected frequencies did not have overlapping harmonics. Because the experimental paradigm was designed so that peak displacement amplitude was held constant, peak velocity of the stimulus co-varied with frequency (Table I).

D. Analyses

1. Phase-planes with Poincaré sections

Linear excursions of the infrared markers were sampled at 100 Hz from which angular displacement of the head in the sagittal plane was calculated. To remove any linear trends in the data, a least-squares fit was performed on the expeimentally recorded time series for angular position and angular velocity and the resulting function was subtracted from the data. Root mean square (rms) values and standard deviations of linearly detrended angular velocity and angular position signals were calculated across the period of the trial. Linear characteristics of the system were identified by defining the transfer function between the trunk displacement in the *x*-direction as the input and the head angular displacement in the vertical plane as the output (refer to Fig. 1 and Table I).

To assess the potential impact of bite bar vibrations on the stabilizing effect of the stimulus parameters on head–neck dynamics, a third order low pass digital Butterworth filter was used to filter the angular velocity signal. Spectral density data demonstrated high frequency noise was present in the velocity data in response to the 0.81 Hz perturbation (Fig. 5), accordingly only that data was filtered. To explore the effect of cut-off frequency on our results, three different cut-off frequencies (50 Hz, 10 Hz, and 5 Hz) were used on both the angular position and angular velocity data. We did not filter more stringently than 5 Hz because we did not wish to filter out the natural frequency responses of the head.[7] We found that severely filtering out high frequency noise did not

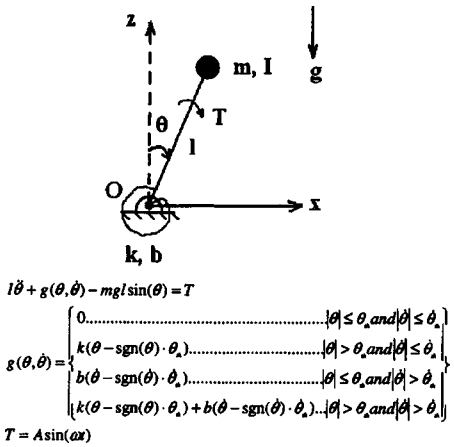

FIG. 2. The system is modeled as an inverted pendulum where m=mass and I=moment of inertia about the joint (O), and T=input torque. Total stiffness and damping around the joint are modeled as k and b, respectively. Simulations performed with this model demonstrate that, for small amplitude perturbations, the system acts in a linear fashion about the gravitational vertical. Thus nonlinear behaviors of the system for small amplitude motion are not due to the geometry of the system. Two nonlinear sources (θ_{th}, $\dot{\theta}_{th}$) were used to model receptor thresholds using a stationary dead-zone that depended upon angular position and angular velocity.

alter the direction of the results (i.e., the sign of the Lyapunov exponent as a function of frequency/amplitude of the stimulus).

Phase-plane diagrams for revealing system dynamics were constructed by plotting head angular position against head angular velocity. Poincaré sections were taken from the phase-plane representation with respect to the initial sled position. Our experimental paradigm was based on holding the peak perturbation displacement constant so that a positional reference was used in order to ensure that the Poincaré section was placed on the first returning phase point. Variability of the phase points at each Poincaré section was computed as a measure of dispersion.[17]

A Poincaré section is the plane perpendicular to the flow direction of the dynamics represented on the phase plane. Points at which the trajectories hit the plane at every driving period of the system are marked. When a Poincaré section is taken through the phase-plane representation it always passes through the same phase point. The point that the trajectories hit the Poincaré section is an estimate of diverging or converging dynamics generally expressed as Lyapunov exponents.[18,19] Positive Lyapunov exponents are associated with divergence (better known as a chaotic behavior) and negative exponents are a measure of convergence (a stable behavior). To quantify system dynamics at the phase-plane we determined the sign of the largest Lyapunov exponent calculated across the period of the trial.[19,20]

To illustrate the Poincaré method of analysis used in this study, a single degree-of-freedom model, an inverted pendulum, was simulated first with a position threshold nonlinearity and then with both position and velocity sensor threshold nonlinearities. The nonlinear equation of motion and the nature of the threshold nonlinearity is shown in Fig. 2 and explained in detail in the legend.

2. Statistical analyses

For the experimental data, we compared the standard deviations of the full dataset and the Poincaré sections to quantify the spatial–temporal irregularity of the system (Table I). Within subject significant differences were tested with t-tests at a $p<0.05$ level corrected for multiple testing. If the emergent response suggested a chaotic system, then we would expect the standard deviation at the Poincaré sections and of the full dataset to be equal. With a stable system, the standard deviation at the Poincaré section should be much less than that of the full dataset.

RMS values of the head angular velocities across perturbation frequencies and transfer function magnitudes for each perturbation frequency and amplitude were compared with multiple t-tests for paired samples at the confidence level of $p<0.05$. A Bonferroni adjustment was used to correct for multiple comparisons.

The primary variable of interest in this study is the sign of the largest Lyapunov exponent (LLE) which indicates whether the system is presenting chaotic (positive sign) or stable (negative sign) behavior. To determine changes in the sign of the LLE with amplitude and frequency, a nonparametric two-sided sign test was applied to the estimated LLE from the filtered and unfiltered data at 0.81 Hz (first column in Table II), and to the unfiltered data at 1.76 and 2.25 Hz with the confidence level of $p<0.05$. Comparisons done on the differently filtered data at 0.81 Hz was conducted to eliminate the potential contribution of bite-bar vibrations.

III. RESULTS

A. Exemplar model simulations

The system described in Fig. 2 was simulated for both a high (2.25 Hz driven by 0.8 N m) and low (0.81 Hz driven by 0.1 N m) frequency/velocity pair of input torques with thresholds set only for receptor position. Model parameters were modified to match reported values in the physiological range of the mass and total stiffness of the head–neck complex,[21] and the resonance frequency of the system was set near 2 Hz.[1] The results of the simulations are shown in Figs. 3 and 4 using the system parameters defined in the legend. It is clear from the phase–plane portrait shown in Fig. 3(c) that variability in position and velocity are present at any Poincaré section (i.e., there is a large standard deviation of 13.46 deg/s between sections). The reason for this variability is the spatial–temporal irregularity (dispersion) of the chaotic function.[17] Moreover, the LLE was positive (0.5 in 1/s), which is an indication of chaotic behavior.[20]

When angular velocity was increased by increasing the frequency of perturbation, the system was stimulated above threshold (Fig. 4). Phase points at the Poincaré section are relatively stationary (i.e., there is a small standard deviation of 4.01 deg/s between sections) with respect to the curve indicating a stable response [Figs. 4(a) and 4(b)]. The resultant stable response was described by a negative value of −9 in 1/s for the LLE. This was a highly ordered system where an elliptical trajectory corresponded to a sine wave while the

TABLE II. Largest Lyapunov exponents of the subjects for the perturbation parameters applied.

Subjects[a]	Peak displacement amplitude: 15 mm Perturbation frequency (Hz)			Peak displacement amplitude: 25 mm[d] Perturbation frequency (Hz)		
	0.81[c]	1.76	2.25[c]	0.81	1.76	2.25
1 (F)	[b]0.82/0.70/0.03	1.00	0.80	[b]0.15/0.08/0.02	0.20	−0.06
2 (M)	0.40/−0.25/−0.27	−1.00	−0.30	−0.15/−0.20/−0.25	−0.07	−0.08
3 (M)	−0.05/−0.07/−0.02	0.25	−0.45	−0.10/−0.08/−0.23	−0.95	−0.20
4 (F)	0.20/0.08/0.20	−1.15	−0.65	0.30/0.15/0.02	−0.40	−0.85
5 (F)	0.35/0.13/0.15	0.15	−0.30	0.18/0.15/0.08	0.97	−0.20
6 (F)	0.95/0.43/0.05	−1.40	−0.23	−0.37/−0.40/−0.33	−2.90	−1.70
7 (F)	−1.27/−1.25/−1.60	−0.14	0.44	−0.14/−0.17/−0.30	−0.90	0.04
8 (M)	0.70/1.10/0.28	0.67	−1.80	−0.25/−0.05/−0.50	−1.84	−1.00
9 (M)	−0.02/−0.18/−0.12	−3.00	−2.90	0.34/0.55/0.30	−2.10	−0.50
10 (F)	1.10/0.90/0.75	−1.35	0.25	0.57/0.50/0.60	−0.65	−0.75
11 (M)	−0.30/−0.31/−0.30	0.80	−1.50	−0.14/−0.30/−0.10	−0.60	−0.40
12 (F)	1.00/0.35/0.12	2.75	−4.65	−0.18/−0.10/0.10	0.20	3.60

[a](F)=female and (M)=male subjects.
[b]LLEs computed at 0.81 Hz for each of the peak displacement amplitude are presented for data that has been unfiltered and digitally filtered with a cut off frequency at 10 Hz and 5 Hz, respectively.
[c]Sign of the largest Lyapunov exponents (LLE) in (1/s) present significant differences with respect to the frequency of perturbation ($p < 0.006$).
[d]Significantly greater number of negative LLEs in (1/s) across frequencies ($p < 0.01$).

center of the ellipse was a stable equilibrium point. The unchanging sinusoidal response is portrayed as a single phase point at its Poincaré section [Fig. 4(c)].

Although, angular excursions of the system for the two different frequencies at the same amplitudes are not considerably different, the angular velocities however are different. With low frequency (low angular velocity) there is sufficient time during a single cycle for $g(\theta, \dot{\theta})$ to take 2 possible values (zero or nonzero depending on the positional threshold), hence changing its contribution to the stabilization of the system dynamics against gravitational pull within a cycle. This contribution could fluctuate between stimulus cycles, resulting in variation in cycle characteristics. On the other hand, at high frequencies (with higher velocities), the contribution of $g(\theta, \dot{\theta})$ to the overall system dynamics is more stable within a cycle than other nonlinear dynamics of the system (e.g., the gravity term) which results in minimizing the cycle to cycle variability, thus stabilizing the Poincaré sections.

B. Experimental data

Angular displacement and angular velocity of the head in the sagittal plane is shown for one subject across a 20 s period of the trial in response to the 0.81 Hz [Figs. 5(a) and 5(b)] and a 10 s period in response to the 2.25 Hz [Figs. 6(a) and 6(b)] sine waves. Although the amplitude of the stimulus is the same for both frequencies (15 mm), it is clear from the figures that the excursion of the head is not the same at both frequencies (see also Table I). Also, at 0.81 Hz, an angular head oscillation is exhibited on the order of 1°–2° peak to peak. Irregular, long term oscillatory behavior (low frequency component <0.3 Hz) about the initial position determined by the laser pointer was observed across the whole time series on the order of approximately 10°–15°. This low

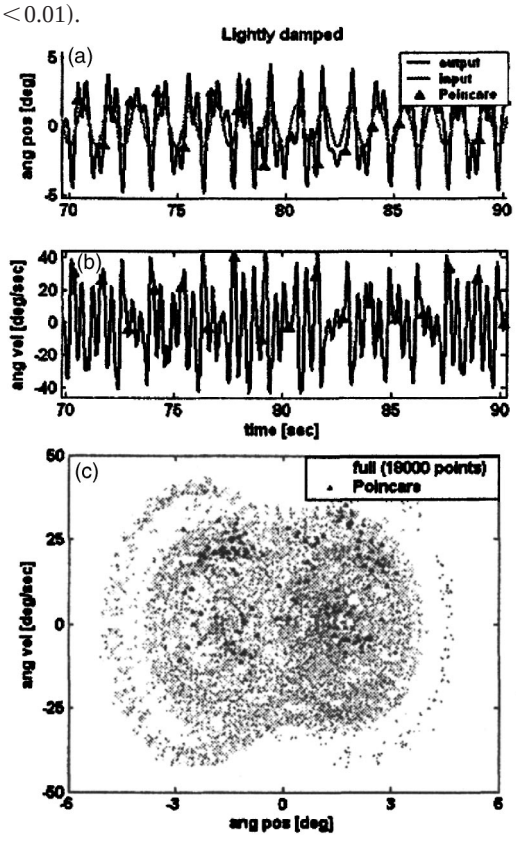

FIG. 3. Output of the model simulation for a lightly damped system by using published physiological parameters for the head and neck (Ref. 21). Input parameters for a lightly damped system with a driving frequency of 0.81 Hz were: $T=0.1$ N m, $m=4.5$ kg, $k=10$ N m/rad, $b=0.01$ N ms/rad, $\theta_{th}=1°$, $\dot{\theta}_{th}=0°/s$. Moment of inertia with respect to the center of mass (I) and the length (l) were: 0.0233 kg m^2 and 0.07 m, respectively. Time step for numerical integration was 0.01 s for all simulations and the simulations lasted for 180 s. The top plot (a) presents a 20 s period of the angular position of the simulated input and output. The middle plot (b) presents a 20 s period of the angular velocity of the simulated input and output. Poincaré section points are shown as triangles on each output trace. The bottom plot (c) is the phase plane representation of angular position and velocity across the period of the trial.

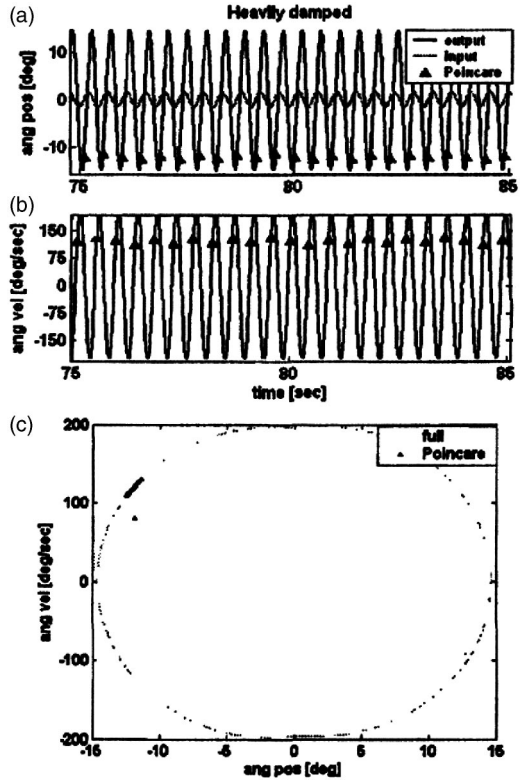

FIG. 4. Output of the model simulation for a heavily damped system with a driving frequency of 2.25 Hz. Plots are the same as in Fig. 3. Input parameters were: $T=0.8$ N m, $m=4.5$ kg, $k=10$ N m/rad, $b=0.2$ N ms/rad, $\theta_{th}=1°$, $\dot{\theta}_{th}=0°/s$. 10 s period of simulations are presented in (a) and (b).

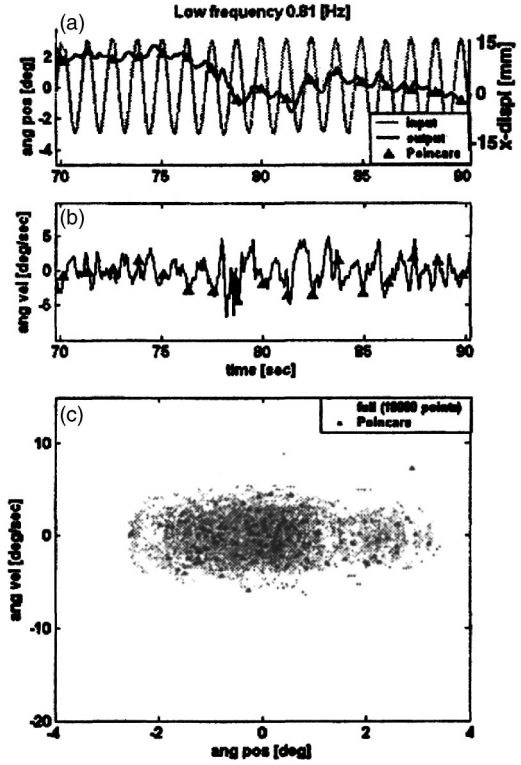

FIG. 5. Head angular position and velocity data from one subject across a 20 s period of a trial with a 0.81 Hz input. Trunk linear position is plotted on the top graph in arbitrary units (gray line). Poincaré section points are shown as triangles on the head angular position (a) and head angular velocity (b) traces. The bottom plot (c) is the phase–plane representation of angular position and velocity across the period of the trial. The number of data points used to construct the phase plane is 18 000. Poincaré section points are plotted as triangles.

frequency oscillatory behavior in head angular excursion was very consistent across all subjects at 0.81 Hz. Moreover, transfer function magnitudes were considerably lower at 0.81 Hz compared to the 1.76 and 2.25 Hz frequencies for both amplitudes of the stimulus (Table I). However, the head angular response increased with stimulus frequency at 1.76 Hz and differed significantly with respect to peak displacement of the perturbation amplitude ($p<0.001$). Because the experimental paradigm was designed to hold perturbation amplitude constant, peak velocity and acceleration of the stimulus co-varied with perturbation frequency (Table I). Mean value of the RMS head angular velocity across subjects was significantly smaller ($p<0.004$) at 0.81 Hz than at the other two frequencies at both peak displacement amplitudes (Table I), and head angular velocities were smaller at 1.76 Hz than at 2.25 Hz for both perturbation amplitudes. In all subjects, peak head angular velocity did not increase with increased peak velocity and amplitude of the stimulus at 0.81 Hz. But head angular velocity did increase with sled velocity almost proportionally for the two higher perturbation frequencies at both peak displacement amplitudes (Table I). Thus the response of the head appears to be uncorrelated with the parameters of the sine wave at 0.81 Hz [Figs. 5(a) and 5(b)] but becomes better coupled to the input at increased frequencies [Figs. 6(a) and 6(b)].

In the bottom graphs of Figs. 5 and 6, head angular position was plotted against the corresponding head angular velocity at two frequencies to obtain the phase-plane diagrams. Standard deviations (SD) of head angular position and velocity for the entire phase plot were compared to those of the Poincaré section to quantify spatial–temporal irregularity. At 0.81 Hz, there were irregular trajectories and a diffuse Poincaré section suggesting an aperiodic bounded response with multiple equilibrium points [Fig. 5(c)] at both amplitudes (15 mm and 25 mm). Further analysis of the LLE showed positive values in 8 out of 12 subjects for the 15 mm perturbation and 5 out of 12 subjects for the 25 mm perturbation (Table II).

The global picture of the head and neck system response was different for the higher frequency inputs. Trajectories of the phase–plane displayed almost periodic oscillations and Poincaré sections exhibited clustered phase points [Fig. 6(c)]. Comparison of the standard deviation across the entire trial period to the Poincaré section at each frequency found significantly lower spatial–temporal irregularity for the 1.76 and 2.25 Hz perturbations for both angular position and angular velocity ($p<0.004$ for both). The data imply that these responses were not likely to be chaotic and, accordingly, the LLE was found to be negative in six subjects at 1.76 Hz and 9 subjects at 2.25 Hz for the 15 mm perturbations. Negative Lyapunov exponents were also found in nine subjects at 1.76 Hz and 10 subjects at 2.25 Hz for the 25 mm perturbations.

The general outcome of the statistical analysis demonstrates that although there is variability within each amplitude across frequencies and across subjects (Table II), the

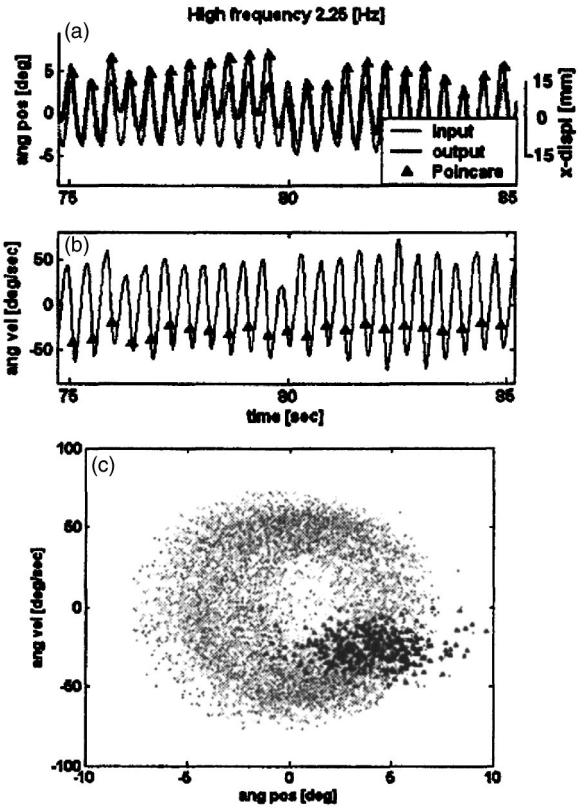

FIG. 6. Data from the same subject data for a trial at 2.25 Hz for a 10 s period.

general direction of the LLEs was to decrease toward a more stable behavior (more negative values) as a function of increased amplitude ($p<0.01$). This outcome was independent of which filtering frequency was used on the 0.81 Hz data as indicated by the nonparametric sign test which did not demonstrate any statistically significant effect (Table II).

The effect of frequency within each amplitude, however, was not as clear. Within the 15 mm peak displacement, there was a significant shift toward increased stability of the head when the perturbation frequency increased from 0.81 to 2.25 Hz ($p<0.006$) (Table II). Exceptions to this pattern were exhibited by the first subject who was unstable for all three stimulus frequencies and presented a chaotic response described by positive LLEs. The seventh subject presented stable responses at 0.81 and 1.76 Hz but was unstable at 2.25 Hz perturbation. The tenth subject produced a chaotic response at 0.81 and 2.25 Hz but exhibited a stable response at 1.76 Hz.

Within the 25 mm peak displacement, only one subject (subject 12 in Table II) exhibited a chaotic response as the perturbation frequency increased from 0.81 to 2.25 Hz. The rest of the subjects exhibited increased stability with increased frequency (although the seventh subject was at most marginally stable). The significant difference in the sign of the LLE between 0.81 Hz and 2.25 Hz disappeared with the larger displacement amplitude, suggesting that the system exhibited increased stability across all frequencies at this amplitude of perturbation. Indeed, a sign test applied across the frequencies within each of the displacement amplitude revealed that there were significantly more negative than positive LLEs only with 25 mm of peak displacement ($p<0.01$).

C. Simulation of experimental data

To further investigate whether sensory threshold and non-linear mechanics contributed to nonlinearities observed in the experimental data, we examined whether the simplistic model shown in Fig. 2 could explain the experimental findings. Our initial simulations of the model with the position dependent sensory function only [i.e., $g(\theta,\dot{\theta})=g(\theta)$] (Figs. 3 and 4) did look similar to the low frequency experimental data [Fig. 5(c)], but did not fit the higher frequency results [Fig. 6(c)]. As shown in Fig. 6(c), phase–plane representations of the experimental data at the higher frequency perturbations resulted in relatively scattered points at the Poincaré section. LLEs derived from the experimental data indicate that the system exhibited varied levels of stability (Table II) and, in some cases, was close to unstable behavior at the higher perturbation frequencies (range of -0.06 to -4.65 LLE in $1/s$). In fact, the LLE in three subjects at 15 mm and 2 subjects at 25 mm peak displacement amplitudes was found to be positive at the highest frequency of perturbation (Table II). In contrast to the experimental data, simulation results [Fig. 4(c)] were highly stable at the higher frequency inputs (as seen by a considerably negative LLE of -9 $1/s$). A velocity/position sensory function was then incorporated into the model [i.e., $g(\theta,\dot{\theta})=g(\theta,\dot{\theta})$]. With both position and velocity thresholds incorporated (see Fig. 7), model simulations at higher perturbation frequencies resulted in a less negative value of the LLE (-0.03 in $1/s$) pushing the system closer to instability. Hence, the inclusion of the velocity threshold component produced a better match to the experimental data at both low and high frequency perturbations.

IV. DISCUSSION

The description of multidimensional musculoskeletal systems, such as the head, neck, and trunk, is complex because of the inertial, Coriolis, centripetal, and gravitational forces arising from the dynamic interaction between different segments (head and trunk motion), and the interjoint moments produced by muscular contractions of voluntary or reflex origin.[22] Furthermore, nonlinear properties of the tissue and joint response characteristics add to the complexity of the system. But most models of head–neck stabilization have relied principally on linear dynamical modeling.[23] The justification for this approach has been that as long as small amplitudes of perturbation were employed, we were acting within a linear response window.[1] Linear lumped parameter models with greatly simplified kinematics have been able to explain the behavior of the head and neck when the primary control system was reflexive in nature.[8,24,25] Departures from model predictions arose, however, when behaviors incorporating both reflex and voluntary control systems were being tested. There was often intersubject variability that could not easily be explained by simply shifting model parameters.[1,6,9,26]

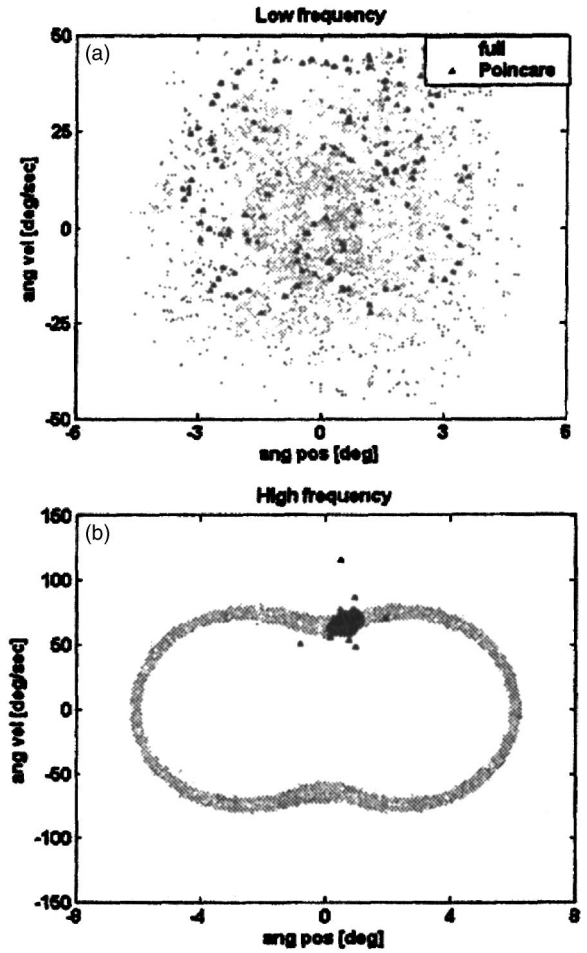

FIG. 7. Output of the model simulation with both of the thresholds having nonzero values. (**a**) Phase–plane representation of simulated response to a 0.81 Hz input. Input parameters were: $T=0.1$ N m, $m=4.5$ kg, $k=10$ N m/rad, $b=0.01$ N ms/rad, $\theta_{th}=1°$, $\dot{\theta}_{th}=80$ deg/s. (**b**) Simulated response to a 2.25 Hz input. Input parameters were: $T=0.8$ Nm, $m=4.5$ kg, $k=20$ N m/rad, $b=0.2$ N ms/rad, $\theta_{th}=1°$, $\dot{\theta}_{th}=80$ deg/s. Both are representing 180 s long simulations and contain 18 000 points of data.

The principal result of this study indicates, however, that increasing the amplitude of the perturbation had a stabilizing effect on the behavior of the head across both frequencies and subjects and exhibiting a more linear response. On the other hand, frequency response and phase–plane analyses performed here suggest that the response variability observed within the small amplitude perturbations is due to nonlinear frequency dependent behavior of the head–neck system.[5,26,27] Such behavior was seen in subjects fluctuating between stability and instability across frequencies. The pattern that emerged in the individual head dynamics of the subjects within amplitude and increasing frequency, and in the overall responses quantified by the Lyapunov exponents, might be explained as chaotic determinism.[28]

Our simulations suggest that the deterministic element in this paradigm was the neural component of the head–neck system, specifically the position and velocity thresholds of system receptors. In our experimental paradigm, amplitude was held constant while frequency and velocity co-varied. For each of the stimulus amplitude we observed significant effects of frequency in our simulations. When only a position threshold was included in our model, the low frequency responses were described, but variability in the higher frequency effects could not be explained. When a velocity threshold was also incorporated, the model simulation more closely matched the overall pattern of behavior and the largest Lyapunov exponents computed for the system over the frequency spectrum.

In physiological systems we know that different sensory modalities respond to different frequency bandwidths. For example, in the vestibular labyrinths, the otoliths are predominantly responsive at low frequencies with significant emphasis on position and the semicircular canals are more responsive at higher frequencies to head angular accelerations in space.[10,29,30] In an intact system, sensory information from these receptors is combined with other proprioceptive information derived from vision, cervical joint receptors, and neck muscle spindle receptors.[1,4,12,31] Thus an attempt to include a sensory function that would have position as well as velocity thresholds conceptually conforms to the normal physiological sensory systems involved in head and neck stabilization.[15]

The problem of identifying the correct threshold for the different sensory modalities remains, however. We have not controlled for baseline activation of our system, thus we cannot predict the precise threshold of these receptors. Both animal[31–33] and human[1,6,34] experiments have demonstrated that receptors involved in head–neck control have bandwidths in which they predominantly control system responses. One plausible explanation for the differences between the low and high frequency responses observed in our data is that the receptors may not be recruited in a sequential fashion, but that they are recruited in an overlapping manner and are then variably selected by the CNS for preferential control of the response. At low frequencies there is more time to shift between the available sensors than at high frequencies, and shifting sensory dominance would explain the increased response variability.

Intersubject variability presented by the largest Lyapunov exponents at low frequencies may be due to a difference in each individual's sensory threshold values. Another potential explanation for the greater variability observed at low frequencies is control by voluntary mechanisms which have been shown to dominate system responses at frequencies below 1 Hz.[1,4,6] Higher level processing of low frequency inputs could produce changes in active torque as a result of fluctuations in the subject's attention which was not controlled in these experiments. However, despite the long trial periods, habituation in head position or velocity was not observed[35,36] suggesting either that subjects were continuously engaged throughout the trial or that sensory adaptation did not take place. It is also possible that the variability we observed in our subjects was due to the volitional selection of different response strategies. For example, in seated subjects receiving high jerk linear accelerations with the head free, head stabilizing responses were observed to be distributed on a continuum between two extreme categories—stiff and floppy.[37]

At higher frequencies, the sensory reflex emerges as a predominant control mechanism[1,6,34] that can provide a more

consistent (stationary) response to perturbations.[38,39] Subjects may also rely upon passive system mechanics at higher frequencies.[24] Because the model we used to simulate this behavior was a lumped parameter model, we could not differentiate between the passive and active mechanisms. We might have been able to make a better judgment about this issue if we had collected EMG responses. Our earlier studies suggest, however, that surface EMG recordings were not sufficient to identify stabilizing strategies in the head and neck;[1,6,40,41] subjects could potentially have been using deep, axial musculature to keep the head–neck ensemble in line with the trunk.[42] Nevertheless, further investigation of neck muscle activation is warranted.

Variability in the behavior observed with changing frequencies might also be due to our experimental design. Head angular position and velocity data were collected from sensors attached to a bite-bar and subjects were instructed to maintain a steady state clenching force on the bar. Although we did not perform a calibration between movement of the bite-bar and of the head, previous literature[16] has indicated that using a bite-bar is a reliable method for measuring small vibrations of the head if the mass of the bar falls below 350 g. Our bite bar had a mass of 90 g. Nevertheless, comparisons were conducted to assess the potential effect of bite bar vibrations on the primary outcome variable of this study (the sign of the largest Lyapunov exponent). This was done by filtering the position and velocity data prior to the estimation of the largest Lyapunov exponents using different cutoff frequencies. In general, the sign of the largest Lyapunov exponent was independent of which filtering frequency was used as indicated by the nonparametric sign test (Table II). While, bite bar vibrations may have been present during the data collection, we believe that our main findings were not affected by these vibrations.

We are not certain, however, about the consistency of the clenching force because we did not incorporate a measure of force in our experimental protocol. Fluctuations in the clenching force might have contributed to the response variability observed at low frequencies. It is possible that the clenching force on the bite bar had a greater effect at the higher perturbation frequencies where we would expect forces exerted on the bite-bar to be more consistent as a result of either descending commands producing a neck muscle cocontraction strategy[43] or a change in the excitability of the neck muscle reflexes which would contribute to the stereotypic responses[38,39] observed here.

The results of this study have both a functional and basic scientific significance. As the predominant frequency of head motion during ambulation is about 1.8 Hz,[44] transitions between the nonlinear disordered behavior observed at lower frequencies and the linear periodic behavior occurring with locomotion are likely to occur in daily life. Previous studies of head movement, which have used stochastic inputs[1,4,6,27] may have missed large changes in head stabilization associated with these transitions. It seems that the system can be linearized for a specific set of inputs even if the experimental data for this particular set of input parameters shows high intersubject variability. Nevertheless, a linear model will not identify overall system behavior even in a very narrow spectrum of perturbation frequencies. Although this study has not conclusively pointed toward any single mechanism as responsible for the responses observed, it has revealed clear directions for further investigation. We have used a crude model here that does not specifically include all head and neck dynamics, but it does contain fundamental physiological features found in a neuromuscular model, i.e., sensory threshold and linear mechanics. We conclude that it is not effective to continue with linear analyses of this system given that such analyses would not tap into system variations including sensory pathologies. Future experiments will be necessary to determine the range of input and system parameters at which there are transitions between nonlinear and linear behavior. Identifying these parameters may provide insight about how CNS controllers select response strategies when presented with varying kinematic demands.

ACKNOWLEDGMENTS

Supported by NIH–NIDCD Grant No. DC01125 (E.A.K.) and NIH–NINDS Grant No. NS38286 (T.C.H.).

[1] E. A. Keshner and B. W. Peterson, J. Neurophysiol. **73** (6), 2293–2301 (1995).
[2] G. R. Barnes and B. H. Rance, Aviat Space Environ. Med. **46** (8), 987–993 (1975).
[3] P. Viviani and A. Berthoz, Biol. Cybern. **19** (1), 19–37 (1975).
[4] D. Guitton, R. E. Kearney, N. Wereley, and B. W. Peterson, Exp. Brain Res. **64** (1), 59–69 (1986).
[5] M. Gresty, Mov Disord. **2** (3), 165–185 (1987).
[6] E. A. Keshner, R L. Cromwell, and B. W. Peterson, J. Neurophysiol. **73** (6), 2302–2312 (1995).
[7] E. A. Keshner, J. Neurophysiol. **89** (4), 1891–1901 (2003).
[8] G. C. Y. Peng, T. C. Hain, and B. W. Peterson, Biol. Cybern. **75**, 309–319 (1996).
[9] K. J. Chen, E. A. Keshner, B. W. Peterson, and T. C. Hain, J. Vestib. Res. **12** (1), 25–33 (2002).
[10] J. V. Wilson and J. Melvill, *Mammalian Vestibular Physiology* (Plenum, New York, 1979).
[11] G. D. Paige and S. H. Seidman, Ann. N.Y. Acad. Sci. **871**, 123–135 (1999).
[12] T. Mergner, Current Psychology of Cognition **21**, 129–212 (2002).
[13] T. Mergner and W. Becker, Ann. N.Y. Acad. Sci. **1004**, 303–315 (2003).
[14] S. M. Mcgill, K. Jones, G. Bennett, and P. J. Bishop, Clin. Biomech. (Los Angel. Calif.) **9**, 193–198 (1994).
[15] U. Proske, A. K. Wise, and J. E. Gregory, Prog. Neurobiol. **60**, 85–96 (2000).
[16] G. S. Paddan and M. J. Griffin, J. Biomech. **21** (3), 191–197 (1988).
[17] R. Badii and A. Politi, *Complexity* (Cambridge University Press, Cambridge, 1997).
[18] C. Robinson, *Dynamical Systems* (CRC, Boca Raton, Florida, 1999).
[19] G. L. Baker and J. P. Gollub, *Chaotic Dynamics* (Cambridge University Press, New York, 1990).
[20] A. Wolf, J. B. Swift, H. L. Swinney, and J. A. Vastano, Physica D **16**, 285–317 (1985).
[21] G. C. Y. Peng, Ph.D. dissertation, Northwestern University (1996).
[22] J. R. Lackner and P. A. DiZio, Trends in Cognitive Science **4** (7), 279–288 (2000).
[23] B. W. Peterson, Prog. Brain Res. **143**, 369–381 (2004).
[24] E. A. Keshner, T. C. Hain, and K. J. Chen, J. Vestib. Res. **9** (6), 423–434 (1999).
[25] B. W. Peterson, J. F. Baker, J. Goldberg, and J. Banovetz, Prog. Brain Res. **76**, 163–172 (1988).
[26] *The Head–Neck Sensory Motor System*, edited by A. Berthoz, P. P. Vidal, and W. Graf (Oxford University Press, New York, 1992).
[27] M. A. Fard, T. Ishihara, and H. Inooka, J. Biomech. Eng. **125** (4), 533–539 (2003).
[28] K. H. Chon, J. K. Kanters, and R. J. Cohen, and N. H. Holstein-Rathlou, Physica D **99**, 471–486 (1997).

[29]G. D. Paige and S. H. Seidman, Ann. N.Y. Acad. Sci. **871**, 123–135 (1999).
[30]D. E. Angelaki, D. M. Merfeld, and B. J. M. Hess, Exp. Brain Res. **132**, 539–549 (2000).
[31]J. Goldberg and B. W. Peterson, J. Neurophysiol., **56** (3), 857–875 (1986).
[32]B. W. Peterson, J. Goldberg, G. Bilotto, and J. H. Fuller, J. Neurophysiol., **54** (1), 90–109 (1985).
[33]G. Bilotto, R. H. Schor, Y. Uchino, and V. J. Wilson, Brain Res. **238** (1), 217–221 (1982).
[34]E. A. Keshner and B. W. Peterson, Prog. Brain Res. **76**, 329–339 (1988).
[35]J. S. Blouin, M. Descarreaux, A. Belanger-Gravel, M. Simoneau, and N. Teasdale, Exp. Brain Res. **150**, 458–464 (2003).
[36]G. P. Siegmund, D. J. Sanderson, B. S. Myers, and J. T. Inglis, J. Biomech. **36**, 473–482 (2003).
[37]N. Vibert, H. G. MacDougall, C. de Waele, D. P. D. Gilchrist, A. M. Burgess, A. Migliaccio, I. S. Curthoys, and P. P. Vidal, J. Physiol. (London) **532.3**, 851–868 (2001).
[38]T. R. Nichols and J. C. Houk, Science **181**, 182–184 (1973).
[39]P. M. Rack and D. R. Westbury, J. Physiol. (London) **240** (2), 331–350 (1974).
[40]E. A. Keshner, T. C. Hain, and K. J. Chen, J. Vestib. Res. **9** (6), 423–434 (1999).
[41]E. A. Keshner, M. H. Woollacott, and B. Debu, Exp. Brain Res. **71** (3), 455–666 (1988).
[42]E. A. Keshner, K. D. Statler, and S. L. Delp, Exp. Brain Res. **115** (2), 257–266 (1997).
[43]T. Torisu, Y. Yamabe, N. Hashimoto, T. Yoshimatsu, and H. Fujii, J. Oral Rehabil. **28**, 1144–1152 (2001).
[44]E. Hirasaki, S. T. Moore, T. Raphan, and B. Cohen, Exp. Brain Res. **127** (2), 117–130 (1999).